# Density-functional study of magnetism in bare Au nanoclusters: Evidence of permanent size-dependent spin polarization without geometry relaxation

R. J. Magyar
*Interdisciplinary Network of Emerging Science and Technologies (INEST) Group Postgraduate Program, Philip Morris USA, 4201 Commerce Road, Richmond, Virginia 23234, USA and NIST Center for Theoretical and Computational Nanosciences (NCTCN), 100 Bureau Drive, MS 8380, Gaithersburg, Maryland 20899, USA*

V. Mujica
*INEST Group Postgraduate Program, Philip Morris USA, 4201 Commerce Road, Richmond, Virginia 23234, USA; Center for Nanoscale Materials, Argonne National Laboratory, Argonne, Illinois 60439, USA; and Northwestern University, Department of Chemistry, 2145 Sheridan Road, Evanston, Illinois 60208, USA*

M. Marquez
*Research Center, Philip Morris USA, 4201 Commerce Road, Richmond, Virginia 23234, USA; Harrington Department of Bioengineering, Arizona State University, Tempe, Arizona 85280, USA; and NIST Center for Theoretical and Computational Nanosciences (NCTCN), 100 Bureau Drive, MS 8380, Gaithersburg, Maryland 20899, USA*

C. Gonzalez
*Computational Chemistry Group and NIST Center for Theoretical and Computational Nanosciences (NCTCN), 100 Bureau Drive, MS 8380, Gaithersburg, Maryland 20899, USA*

(Received 10 October 2006; revised manuscript received 25 January 2007; published 19 April 2007)

Magnetism in bare uncapped gold nanoclusters is explored from a density-functional theory perspective with scalar relativistic effects included via the pseudopotential. The computed electronic structures of various nanoclusters reveal that permanent size-dependent spin polarization appears without geometry relaxation for bare clusters even though bulk gold is diamagnetic. The polarized ground states for clusters are favorable due to the hybridization of the *s* and *d* orbitals, and bare octahedral clusters are expected to be magnetic for cluster sizes of approximately 38 atoms and larger. Much larger clusters will be diamagnetic when the surface-to-volume ratio is small and the core diamagnetism prevails. Moderate changes in the interatomic distances and cluster geometry are shown not to alter this conclusion. Contrary to local-density approximation and embedded atom method predictions, generalized gradient approximation and hybrid geometry optimizations reveal increased interatomic bond distances in bare gold clusters relative to the bulk lattice values. In this case, optimization enhances the spin polarization.

DOI: 10.1103/PhysRevB.75.144421 PACS number(s): 75.75.+a, 75.20.−g, 73.22.−f, 31.15.Ew

## I. INTRODUCTION

Modern synthesis and characterization techniques have enabled the controlled production of nanosized metal and semiconductor clusters. Because of their small size, these nanoclusters exhibit adjustable optical and physical properties that may differ drastically from their bulk properties. Since these properties often depend critically upon the size and shape of the nanocluster, it is possible that through synthesis, nanoclusters can be tuned to be suitable for precise technological applications. In particular, it would be highly advantageous to fashion nanoparticles with tunable optical, magnetic, and electron-transport properties. This combination would be particularly useful in targeted drug delivery schemes as well as for imaging and diagnosis biomedical applications. For example, the nanoparticles could be injected into a patient, and the concentration of the nanoparticles could be localized in a region of interest by an external magnetic field. Finally, radiation tuned to the particles' plasmon modes could thermally activate the particles resulting in local heating that could, for example, kill undesirable cells.[1] Gold forms a nanoparticle with promising optical and magnetic properties.[2] It is enticing for medical applications because it is both easy to manipulate and is generally considered to be chemically inert, although the latter must be carefully re-examined as a function of cluster size. A very different yet important application is in spintronic technologies and in digital memory devices.[3]

Despite conflicting experimental results, there is a consensus that gold nanoparticles with approximately hundreds of atoms can retain a magnetic moment under zero-field bias. Furthermore, their plasmon range is proportional to the size of the nanoparticle.[2] If both of these conditions are satisfied and controllable, gold would be an even stronger candidate for the aforementioned applications. Understanding what causes this magnetism will be required to exploit, to full advantage, this magnetic behavior in future applications.

Gold magnetism was first observed by Zhang and Sham who used x-ray spectroscopy techniques on alkane-thiolated nanoclusters.[4] A subsequent experiment by Crespo *et al.*[5] used x-ray-absorption near-edge structure to show that, in thiolated clusters on the order of 100 atoms, the gold clusters

 

exhibit a magnetic moment per atom of $\mu=0.036\mu_B$, where $\mu_B$ is the Bohr magneton ($9.27\times10^{-24}$ J/T). In both experiments, magnetism was detected when sulfur-based capping ligands were used, and this led Crespo *et al.* to conclude that ligand-cluster interactions might play a vital role in inducing magnetism. Based on this hypothesis, optical properties could be controlled by choosing the size of the cluster while magnetic properties seemed to be the result of the coverage of sulfur-based capping ligands. It should be noted that neither of these experiments were able to demonstrate magnetism in gold clusters capped with weakly interacting nitrogen-based ligands instead of strongly interacting sulfur-based ligands such as thiolates. This negative result is seemingly in contradiction with the results reported by Foa Torres *et al.*[6] obtained using x-ray magnetic circular dichroism spectroscopy. They found that the presence of magnetism depended strongly on the type of the surfactant and that the magnetism was much stronger for nitrogen-based ligands. They claimed that the strong covalent bond between sulfur and gold induces a spin-singlet state and actually quenches magnetism. They concluded that gold clusters are intrinsically magnetic and that capping ligands could quench this. Hori *et al.* went on to measure the magnetic moment as a function of cluster size, showing that magnetism is indeed a size-tunable property in these systems.[7,8]

There have already been several attempts to model gold nanoclusters theoretically from first principles.[9–20] The difficulty with these theoretical techniques is manyfold. First of all, it is unclear how well these nanoclusters are experimentally characterized in terms of homogeneity, size, and consistency. Second, given the size of a cluster, the exact arrangement of the atoms is uncertain. Third, the achievable accuracy of the computational methods is constrained by the large number of atoms that must be considered to approach typical sizes of clusters seen in experiments. Additionally, computer time and capability limit the size of the clusters that can be modeled. To avoid several of these complications, the vast majority of the theoretical work has been done on smaller clusters ($<$20 atoms), where theoretical methods can be performed exhaustively. For example, Arratia-Perez *et al.*[9] demonstrated the importance of relativistic effects on $Au_{13}$ clusters by performing all electron calculations using the Dirac scattered wave method. Later work on $Au_{13}$ demonstrated that spin-averaged scalar relativistic theory was quite adequate to reproduce the correct level spacings[10] in all electron calculations. Hakkinen *et al.*[11] have performed electronic structure calculations and geometry optimizations on gold cluster anions of up to 14 atoms using density-functional theory (DFT) with a relativistic norm-conserving pseudopotential. According to their calculations, clusters up to $Au_{12}^-$ have planar ground-state geometries in agreement with experiments. Further, they showed that all neutral clusters with even numbers of atoms smaller than $Au_{14}$ have closed shells as evidenced by a gap between the lowest-binding-energy peak and the rest of spectrum.[12] Having closed shells implies no magnetization. This, as we will show later, does not hold in the case of larger gold clusters. Wang *et al.*[13] used the local-density (LDA) in the form of PW91 with a double zeta basis set and a scalar relativistic pseudopotential to find lower-energy amorphous geometries relative to more symmetric ones. They noted a variation in the highest occupied molecular orbital-lowest unoccupied molecular orbital (HOMO-LUMO) gaps depending on whether the number of atoms in the cluster was even or odd. The gap was bigger for an even number of atoms in the cluster. This suggests a closed electronic shell and that clusters with an even number of atoms are spin singlets. None of these earlier calculations hinted at the possibility that high spin ground states would also be possible.

For larger clusters, a combination of semiempirical and density-functional theory has been popular. Early work indicated that a truncated decahedral motif seems to include the most energetically favorable clusters.[14,15] Subsequent geometry optimizations of gold nanoparticles of 38 and 55 atoms suggested that asymmetric non-bulk-like geometries are about 0.1 eV lower in energy than the more symmetric candidates.[16–18] Hakkinen *et al.*[19] showed that $Au_{55}$ is icosahedral using hot-electron spectra of gold clusters. All other anions near it are of lower symmetry types. So far, most computational work has been concerned with the shape and composition of the clusters and not on the details of the electronic structure and consequently the total spin. A notable exception is the work by Hakkinen *et al.* who investigated the detailed electronic structure of bare and thiolated $Au_{38}$ using the local-density approximation;[20] however, their work did not consider the spin state of the gold cluster.

In this paper, we use spin-dependent density-functional theory in the scalar relativistic pseudopotential formalism to study the energetic tendency for the gold clusters to spin polarize. We will show explicitly how this spin polarization depends on the cluster size and that surface ligands are not needed to induce spin polarization. We will show through first-principles calculations that gold clusters are intrinsically magnetic due to the hybridization of the atomic orbitals within the scalar relativistic formalism. This result is general for nanosized clusters but does not apply to magnetism of gold surfaces, which is likely induced by a different mechanism such as chemisorption as demonstrated in Ref. 25. Additionally, we demonstrate that moderate changes in the cluster geometry do not overwhelm this magnetism, and it is plausible that this sort of magnetism will exist in more realistic amorphous geometries.

In Sec. II, we discuss the theoretical framework in which we model the electronic structure of these clusters. In Sec. III, we present the main evidence that bare clusters tend to be spin polarized in a certain size regime, and in Sec. IV, geometry relaxation is seen to enhance the magnetization. We conclude with a discussion of implications of this result and foreshadow future work.

## II. MAGNETISM FROM FIRST PRINCIPLES

The two main findings from the computational work thus far have been the need to account for relativistic effects and the possibility of many energetically similar cluster geometries. Relativistic effects are included in this work through the use of a scalar relativistic pseudopotential. Perturbative addition of valence relativistic terms such as spin orbit, mass velocity, and the Darwin term will be investigated in later

work but are not necessary to reveal the underlying orbital-hybridization mechanics since the energy shifts, in general, are smaller than spin coupling.

Using first principles to accurately determine the geometry is a more difficult problem.[14,15] While it is well known that DFT tends to predict accurate geometries for simple molecules and bulk solids, little is known about the relative trustworthiness of DFT for the structures of highly complicated molecules and large metal clusters. Coupled with the large errors possible from the choice of pseudopotential, basis set, and functional, DFT in its current form may not provide highly reliable geometries of gold clusters even at zero temperature. However, DFT should provide reasonably accurate electronic structure predictions. Furthermore, gold clusters must tend to a face-centered-cubic (fcc) bulklike geometry in the large cluster limit, since a large enough cluster will eventually look like a small piece of bulk gold. This has been verified, for example, by Hori *et al.* from x-ray diffraction and transmission electron microscopy for gold nanoparticles of 2.5 nm in diameter.[7] We choose to use prototypes with high symmetry and to model our gold clusters as ideal cleaves from the bulk fcc gold lattice with a room-temperature lattice spacing of 4.08 Å. This naive choice offers an additional advantage in that the results for these cleaved gold clusters are directly comparable to the results in both the bulk and isolated atom limits.

In order to determine the onset of magnetism in the gold clusters, we perform density-functional quantum chemical calculations within the pseudopotential formalism. Magnetism is indicated by a higher spin state being lower in energy than the un-spin-polarized cluster. All results were generated using GAUSSIAN 03.[21,29] The basis sets were chosen to be either single valence plus polarization with the Stuttgart effective core potential (SVP/STUTT) or the double zeta without polarization LANL2DZ, with its respective effective core potential. Both have been used for transition metals with considerable success.[22–24] The SVP basis set consists of 27 basis functions comprised of 55 primitive Gaussians. The LANL2DZ basis consists of 24 basis functions comprised of 44 primitive Gaussians. In both cases, the pure $5d$ and $7f$ basis functions were used.

The density functionals we use are a generalized gradient approximation [PBE (Ref. 26)] and two hybrid functionals (B3LYP,[27] PBE1PBE). For the smaller clusters, the hybrid functionals are perhaps the most likely to be accurate, since the clusters will be more moleculelike. Hybrids are well trusted in chemistry and have become the standard for molecular DFT-based calculations. The hybrid functionals are known to converge more quickly because the longer-range exchange potential will widen the HOMO-LUMO gap. PBE, on the other hand, is designed to be exact in the uniform gas limit, and it might be expected to be reliable in the large cluster limit. A combined analysis using both classes of functionals is particularly necessary when considering larger molecules. If both classes of functionals predict agreeing trends, then our calculations are expected to be reliable given the vastly different derivations of the functionals.

For $Au_{14}$-$Au_{56}$ clusters, we used an ultrafine grid for density integrations, and a fine grid was used in the case of the $Au_{68}$ cluster. The ultrafine grid consists of 73 radial points and 43 028 total points per atom, and the fine grid consists of 56 radial points and 17 039 total points per atom. Throughout, we used tight convergence criteria. Tight convergence means that the energy was converged to at least 1 mHartree and the rms density matrix to less than 1 part in $10^{-8}$. Self-consistent-field convergence often required the use of extra quadratic convergence steps for the SVP/STUTT basis. Geometry optimizations were constrained by symmetry, restricted to the spin-singlet state, and performed using the B3LYP hybrid functional.

## III. SPIN-POLARIZED BARE CLUSTERS

For a single gold atom in the pseudopotential formalism, 60 electrons are designated to be core electrons and the remaining 11 valence electrons form one $S_{1/2}$, four $D_{3/2}$, and six $D_{5/2}$ states. $D$-band splittings are reproduced by DFT.[10] We can expect that our treatment of relativistic effects through a pseudopotential is adequate to reproduce most of the relativistic effects.[30]

On the one hand, bulk gold is diamagnetic with a mostly filled $d$-band and $s$-shell conduction electrons. A small fraction of vacancies in the $d$ band is not sufficient to overcome the diamagnetism of the core electrons in the gold atoms.[5] In comparison, in the atomic limit, the $d$ shell is completely full. As the gold atoms aggregate into a cluster, the atomic shells will hybridize. As a result, the $d$ shells develop vacancies when gold clusters increase in size. The number of vacancies will be proportional to cluster size. At some intermediate size, the number of $d$-shell vacancies will exceed a critical threshold, and a spin-polarized state will have the lowest energy. For larger clusters, the core diamagnetism dominates, and this surface magnetism is suppressed. The completeness of the suppression depends strongly on gold's magnetic screening length.

In order to test this idea of spin polarization in the clusters, we consider highly idealized, isolated, bare, uncharged, single gold clusters with even numbers of atoms. (Clusters with an odd number of atoms will always be paramagnetic due to the unpaired electron.) Since experiments do not give detailed cluster shapes, we build the theoretical clusters out of the known face-centered-cubic lattice of bulk Au. The clusters are constructed by picking atoms enclosed by spheres of a given radius in the face-centered-cubic bulk gold lattice. This gives high-symmetry gold clusters with either an octahedral shape ($Au_{14}$, $Au_{38}$, and $Au_{68}$) or a bond-centered rod ($Au_{28}$ and $Au_{56}$).

For $Au_{38}$ and smaller clusters, we have been able to optimize the geometry within the B3LYP hybrid method and find that uncapped clusters expand upon geometry relaxation. The bare clusters are a good model for alkylated clusters, where there is a weak interaction between the ligand and the surface gold atoms. The effects of strongly interacting ligands such as sulfur will be studied in a later work. The approximate geometries can be relaxed using electronic structure results to optimize the geometry; however, the choice of optimized or approximate geometries should not greatly affect the conclusions about magnetism in these clusters. Nevertheless, we test this proposition at the end of this section.

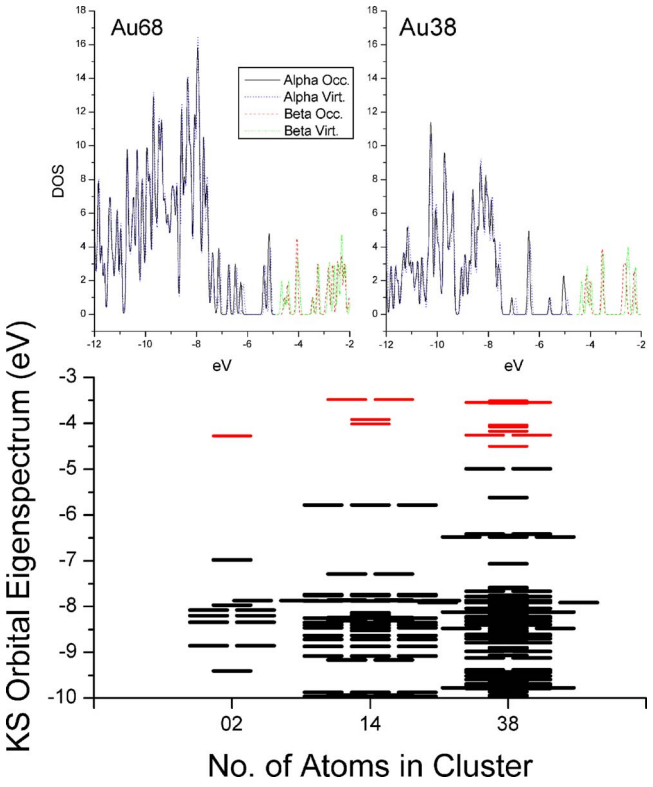


FIG. 1. (Color online) The ground-state spin-dependent density of Kohn-Sham states (DOS) on the top and the singlet orbital Kohn-Sham eigenspectrum (B3LYP/SVP/STUTT) on the bottom. For the orbitals, the solid lines are the occupied Kohn-Sham orbitals, and the gray ones are the unoccupied ones. Degenerate states are indicated by $n$ adjacent lines corresponding to the $n$ degrees of degeneracy. The alpha-spin DOS is marked with circles, and the beta-spin DOS with triangles. The DOS was plotted using gaussian broadening with a 0.05 eV exponential weight factor.

The approximate diameter of the clusters can be obtained from the distance from one surface gold atom to its symmetric partner on the other side of the cluster. For $Au_{14}$, $Au_{38}$, and $Au_{68}$, this gives nonoptimized diameters of 0.71, 0.92, and 1.24 nm, respectively. As $Au_{28}$ and $Au_{56}$ do not have spherical symmetry, we report the largest surface-to-surface distance. This gives nonoptimized sizes of 0.98 and 1.19 nm, respectively. The reader is cautioned, however, that experimental nanoclusters are capped and have charge distributions, which can lead to a much larger effective radii. $Au_{68}$ represents the largest cluster for which we have done calculations in this work.

For the gold dimer, we show the energy levels in the leftmost column of Fig. 1. The HOMO-LUMO gap is 2.6 eV. The symmetry of the occupied orbitals is $s$-like. The unoccupied orbital is also $s$-like. The column on the right-hand side of Fig. 1 depicts the corresponding energy levels for $Au_{38}$. The results in Fig. 1 indicate that the unoccupied band gap vanishes in the case of the $Au_{38}$ cluster, indicating that the spin-singlet ground state is unstable and prefers to decay to a spin-polarized state. Figure 1 demonstrates how the discrete eigenspectrum for gold evolves from the diatomic limit into a bandlike spectrum for the larger $Au_{38}$ cluster. These eigenvalues are determined using the B3LYP functional to calculate the lowest spin ground state (not necessarily the lowest energy) on nonoptimized geometries of neutral gold clusters.

TABLE I. The magnetic moment per atom $[M/n=2\mu_B\sqrt{S(S+1)}/n]$ for different spin states in gold nanoclusters.

| Number of up-down electrons | $Au_2$ | $Au_{14}$ | $Au_{28}$ | $Au_{38}$ | $Au_{56}$ | $Au_{68}$ |
|---|---|---|---|---|---|---|
| 2 | 1.414 | 0.202 | 0.101 | 0.074 | 0.051 | 0.042 |
| 4 | 2.449 | 0.350 | 0.175 | 0.129 | 0.087 | 0.072 |
| 6 | 3.464 | 0.495 | 0.247 | 0.182 | 0.124 | 0.102 |
| 8 | 4.472 | 0.639 | 0.319 | 0.235 | 0.160 | 0.132 |
| 10 | 5.477 | 0.782 | 0.391 | 0.288 | 0.196 | 0.161 |

To find the spin state of a gold cluster, we compare the electronic energy of various spin constrained states. Neglecting possible spin-orbit coupling effects, the magnetic moment of a system is related to its spin by $M=2\mu_B\langle S\rangle=2\mu_B\sqrt{S(S+1)}$, where $\mu_B$ is the Bohr magneton and $S$ is the total spin quantum number. The total spin moment $M$ is divided by the number of atoms $n$ in a cluster ($m=M/n$), and then $m$ is commonly reported in the experimental literature. The experiments are performed at finite temperature, and our calculations are at zero temperature. Table I shows the magnetic moment per atom versus spin state for several clusters we studied. On the left, we list several possible numbers of unpaired electrons for the neutral bare clusters. We arbitrarily stop at ten unpaired electrons. This choice (as we shall present later) is motivated by our theoretical results that show that it is energetically unlikely for gold nanoparticles to become so strongly polarized. Given these values for the numbers of unpaired electrons, the table presents a range of physically possible magnetic moments. The experimentally suggested value of 0.036 $\mu_B$/atom is slightly smaller than the weakest polarized values for each cluster type listed here.

Figure 2 shows a plot of the energy for $Au_{14}$ relative to the lowest-energy electronic spin state. We find that the energetic minimum is spin unpolarized (singlet). This seems to indicate that small bare gold clusters are, as expected, diamagnetic. It also agrees with the naive picture of complete $d$ orbital filling and unbroken symmetry between different spin species. Geometry optimization expands this cluster but does not change the qualitative spin state. This cluster has a very large surface-to-volume ratio with all atoms being surface atoms. Furthermore, all the surface atoms have the same coordination number. It is energetically unfavorable to have holes or localized moments in the $d$ band. A similar result holds for $Au_{28}$ (not shown).

For intermediate sized clusters, a different story unfolds. Figure 3 depicts the relative energy for $Au_{38}$ for various spin polarizations. We find that the energetic minimum (−0.2 eV relative to the spin singlet) is a spin triplet. This minimum is significant even at room temperature of 300 K, where $k_BT=0.03$ eV. Previous calculations on this cluster showed a sixfold degenerate HOMO. Here, we use hybrid functionals and find that the ordering of orbitals has shifted for this cluster, and the HOMO is no longer sixfold degenerate. The spin-

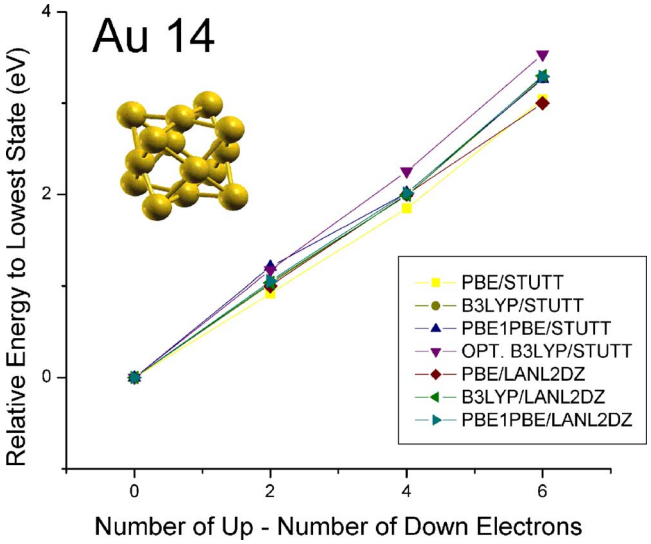


FIG. 2. (Color online) Total energy for the gold $Au_{14}$ nanocluster as a function of the spin state as described via various density-functional methods.

polarized state arises because the atomic orbitals hybridize, and it becomes energetically favorable for holes to form. Geometry optimization enhances the energetic tendency to hybridize and consequently to polarize. The trend is most pronounced for the PBE functional, but also evident in the hybrid functionals. For the larger octahedral cluster, $Au_{68}$, we obtain a similar total-energy curve (Fig. 4). In this case, the energy minimum is only −0.1 eV lower than the singlet, but the lowest-energy state is likely a spin quintuplet. Given

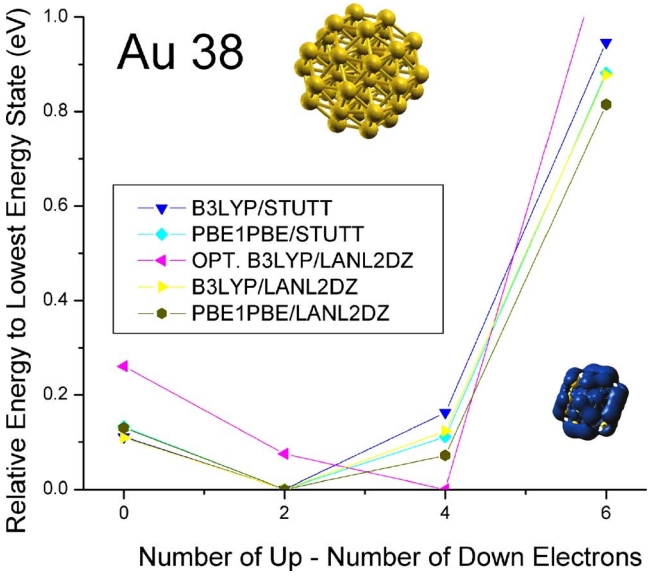


FIG. 3. (Color online) Total energy for the gold $Au_{38}$ nanocluster as a function of the spin state as described via various density-functional methods. The spin polarization for a $Au_{38}$ gold nanocluster (B3LYP/LANL2DZ) is shown in the bottom right. The majority-spin polarization is mostly localized to the surface of the cluster. The diamagnetic core is obstructed by the spin-polarized surface.

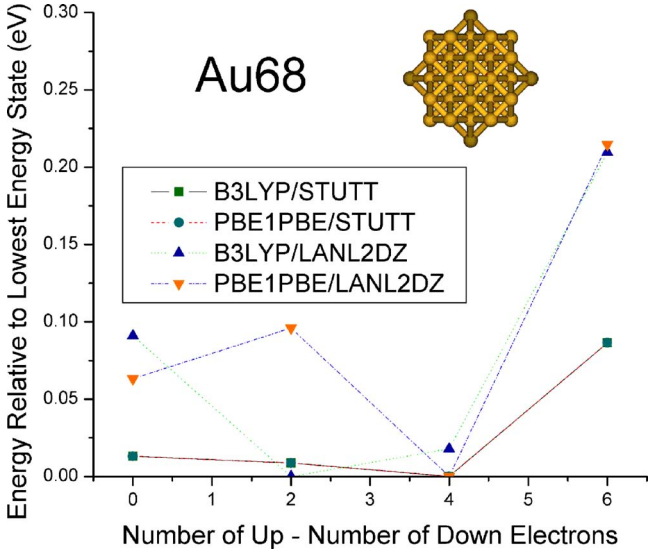


FIG. 4. (Color online) Total energy for the gold $Au_{68}$ nanocluster as a function of the spin state as described via various density-functional methods.

the prohibitive computational expense involved in the use of the ultrafine integration grids for our DFT calculations, a smaller grid was used in the case of $Au_{68}$.

Figure 5 shows the corresponding energy plot for $Au_{56}$. This is a bond-centered cluster and should not be expected to be directly comparable to the same sized octahedral shaped cluster. However, the trends within the set of bond-centered clusters should be similar to the trends seen in the octahedral clusters. The spin-singlet and triplet states are degenerate at our level of theory. For $Au_{28}$, we obtained a spin singlet (not shown), so while this cluster is not large enough to be polarized, it is close to the threshold size at which spin polarization arises.

The electronic spin polarization for the lowest-energy (triplet) state of $Au_{38}$ (B3LYP/LANL2DZ) has been plotted

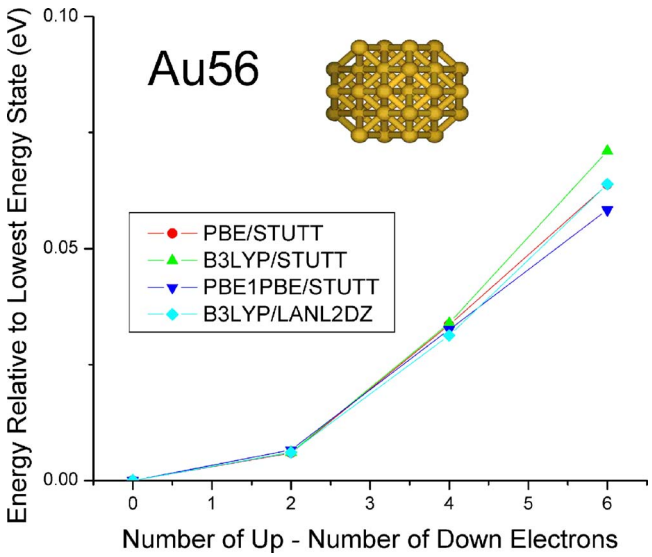


FIG. 5. (Color online) Total energy for the gold $Au_{56}$ nanocluster as a function of the spin state as described via various density-functional methods.

in the lower right-hand corner of Fig. 3. The spin polarization is mostly localized on a surface monolayer of the cluster. A Mulliken analysis of the spin density shows an average of −0.0706 down-spin polarization on each of the six interior atoms and an average of 0.0757 on each of the 32 surface atoms. Thus, the total spin polarization of the surface is 2.42 versus the diamagnetic core with −0.42. A net spin of 2.000 corresponds to the triplet state. The distribution of spin moments is not uniform on the surface, but rather the greatest spin polarization occurs along a plane perpendicular to the $z$ axis. The strong localization to the surface suggests that the magnetism is a surface effect and is likely to be quenched by a strong interaction with capping ligands such as sulfur. An overall interior polarization opposes the strong surface effect. This is consistent with the idea that bulk gold is diamagnetic and that the diamagnetism per atom is weaker than the tendency of the surface atoms to polarize. The core tends to oppose, although weakly, the magnetization of the surface, which is clearly a size-dependent phenomenon.

A similar result is found for the $Au_{68}$ (quintuplet). The spin-density plot is not shown. The surface has eight groups of three gold atoms and six single atom outliers for a total of 30, all with majority spin. The outliers have the highest local spins. The semi-interior atoms (16 atoms) are partially screened from the exterior and have small spins. The interior consists of the 14 atom octahedron and the eight atoms which cap their faces. The core is diamagnetic with the strongest moments on the eight capping atoms. The Mulliken populations of the spin density show an average spin of −0.103 on each of the 14 interior atoms, 0.002 on each of the semi-interior atoms, and 0.180 on each of the 30 surface atoms.

For both the spin-polarized clusters, these results suggest a paradigm of a spin-polarized paramagnetic surface and an antipolarized diamagnetic core.

## IV. GEOMETRY RELAXATION'S ENHANCING EFFECT ON MAGNETISM

For $Au_{38}$ and $Au_{14}$, we have optimized the cluster geometry within the B3LYP/LANL2DZ formalism. Geometry optimization for clusters of these sizes tends to be very expensive. For this reason, we optimized only the singlet ground state and invoked symmetry. For nonsinglets, the geometry will vary slightly; however, it is unlikely that the difference among the various spin-state geometries will be greater than the difference between the initial nonoptimized geometry and the optimized singlet one. Our initial coordinates are the octahedral coordinates from the fcc gold lattice at room temperature and are expected to be slightly expanded relative to coordinates as zero temperature. First-principles calculations are implicitly for an isolated cluster at zero temperature.

We use two measures to compare the relative geometry changes for our clusters. The first is the average rms displacement of a gold atom from the center of mass of the cluster. This can be calculated for both the nonoptimized and optimized clusters. The second measure is the furthest surface-to-surface distance. This gives a rough measure of the diameter, since the physical diameter depends on the electronic charge distribution and is not well defined.

$Au_{38}$ was the only spin-polarized cluster for which we were able to perform geometry optimization. Electronic structure calculations performed on the optimized geometries show curves (Fig. 3) with slightly deeper wells. Since we did not constrain the geometry during optimization, the clusters shifted slightly from the expected octahedral geometries. In order to quantify the relative sizes of the clusters prior to and after geometry relaxation, we compare the average root-mean-squared distance from the center of the cluster.

In our calculations, both clusters expand upon geometry relaxation. This is in contradiction to what is often cited in the literature,[14,15,28] in which a 1% reduction in size relative to the bulk was observed (extended x-ray-absorption fine structure). However, in the reference, the experiment was conducted on thiol-capped nanoparticles. Later measurements by Crespo *et al.*[5] on thiol-capped nanoparticles suggest that they, in fact, do expand from 2.83 to 2.98 Å.

For $Au_{14}$, the average rms value goes from 2.701 to 2.917 Å. This is an 8% increase in size and is consistent with the 5% experimental increase observed by Crespo *et al.*[5] Moreover, there is considerable geometry distortion for the small gold cluster, so while the average rms displacement expands, the longest surface-to-surface distance decreases from 7.067 to 6.888 Å. The optimization and distortion have little if any effect on the magnetic properties of the 14 atom cluster, as seen in Fig. 2.

For $Au_{38}$, we see further evidence of cluster expansion. The rms displacement expands from 3.947 to 4.066 Å, which gives a net expansion of 3%. This result is also in reasonable agreement with the measurements of Crespo *et al.* Considering that strongly interacting ligands such as thiolated ones are expected to cause expansion relative to the bare cluster, the ligands are thought to further expand the clusters, and this too would agree with the experimental results. This cluster has six (100) facets and eight (111) facets. As also seen in previous LDA optimizations of this cluster,[20] the atoms in the center of the (111) facets move outward to make the cluster more spherical. However, the final bond lengths after optimization with the hybrid functional are 5% longer and in the range 2.83–2.95 Å. This is to be expected since LDA typically overbinds systems, and functionals such as hybrids that account for long-ranged exchange correct this.

Despite geometry changes, the magnetic spin state is predicted to be the ground d state at both contracted and expanded geometries. In fact, our data indicate that expansion favors a more strongly magnetized ground state perhaps by encouraging greater hybridization. The furthest distance among surface atoms expands, as well as in this case from 9.123 to 9.235 Å. The $Au_{38}$ cluster exhibits less distortion than the smaller one due to the inner 14 gold atoms, retaining the octahedral structure. Overall, as observed in Fig. 3, full geometry optimization leads to larger magnetization in the cluster, indicating that the conclusions regarding the rise of magnetic behavior in these clusters are not significantly affected by geometry optimization.

## V. CONCLUSIONS

Density-functional calculations presented in this work show that magnetism is, in fact, intrinsic to gold clusters in a

nanosized regime due to atomic-orbital hybridization. The magnetism is localized to a monolayer on the outside of these clusters with the interior regions remaining mostly diamagnetic. These calculations support a paradigm of a spin-polarized paramagnetic surface and a diamagnetic core of opposite and smaller polarization. This arrangement allows for a leveling off of the magnetic moment per atom as the clusters increase in size. For larger clusters, the diamagnetic core will dominate as the surface-to-volume ratio becomes small. Thus, magnetism in gold clusters is primarily a size-dependent effect. The calculations are consistent with the experimental evidence that suggests that magnetism in gold nanoparticles is strongest when weakly interacting capping agents are used. Strongly interacting capping agents would likely quench this magnetic behavior. Future work will examine how sulfur- and nitrogen-based surface ligands affect this result. Preliminary calculations indicate that sulfur does quench the spin polarization by reinforcing the energetic stability of the singlet state. Geometry optimizations within generalized gradient approximation and hybrid density-functional theory indicate that the average interatomic spacings in gold clusters tend to expand relative to the bulk value. However, these geometry changes do not change the qualitative result that bare gold nanoclusters are magnetic in certain size regimes. The next step in our investigation will involve the use of semiempirical tight-binding formulations to obtain better structures followed by single point electronic structure calculations. Since these systems are considered at finite temperature, dynamics must also be considered.

## ACKNOWLEDGMENT

We would like to thank the National Institutes of Health for use of the Biowulf computer cluster.

[1] O. V. Salata, J. Nanobiotechnol. **2**, 3 (2004).
[2] M. Daniel and M. Astruc, Chem. Rev. (Washington, D.C.) **104**, 293 (2004).
[3] S. D. Bader, Rev. Mod. Phys. **78**, 1 (2006).
[4] P. Zhang and T. K. Sham, Phys. Rev. Lett. **90**, 245502 (2003).
[5] P. Crespo, R. Litran, T. C. Rojas, M. Multigner, J. M. de la Fuenta, J. C. Sanchez-Lopez, M. A. Garcia, A. Hernando, S. Penades, and A. Fernandez, Phys. Rev. Lett. **93**, 087204 (2004).
[6] Y. Yamamoto, T. Miura, M. Suzuki, N. Kawamura, H. Miyagawa, T. Nakamura, K. Kobayashi, T. Teranishi, and H. Hori, Phys. Rev. Lett. **93**, 116801 (2004).
[7] H. Hori, Y. Yamamoto, T. Iwamoto, T. Miura, T. Teranishi, and M. Miyake, Phys. Rev. B **69**, 174411 (2004).
[8] Y. Yamamoto and H. Hori, Rev. Adv. Mater. Sci. **12**, 23 (2006).
[9] R. Arratia-Perez, A. F. Ramos, and G. L. Malli, Phys. Rev. B **39**, 3005 (1989).
[10] L. L. Are and F. Ichel-Calendini, Int. J. Quantum Chem. **61**, 635 (1997).
[11] H. Hakkinen, B. Yoon, U. Landman, X. Li, H. Zhai, and L. Wang, J. Phys. Chem. A **107**, 6168 (2003).
[12] H. Hakkinen and U. Landman, Phys. Rev. B **62**, R2287 (2000).
[13] J. Wang, G. Wang, and J. Zhao, Phys. Rev. B **66**, 035418 (2002).
[14] C. L. Cleveland, U. Landman, T. G. Schaaff, M. N. Shafigullin, P. W. Stephens, and R. L. Whetten, Phys. Rev. Lett. **79**, 1873 (1997).
[15] C. L. Cleveland, U. Landman, M. N. Shafigullin, P. W. Stephens, and R. L. Whetten, Z. Phys. D: At., Mol. Clusters **40**, 503 (1997).
[16] I. L. Garzon, K. Michaelian, M. Beltran, A. Amarillas, P. Ordejon, and E. Artacho, Phys. Rev. Lett. **81**, 1600 (1998).
[17] K. Michaelian, N. Rendon, and I. L. Garzon, Phys. Rev. B **60**, 2000 (1999).
[18] E. M. Fernandez, J. M. Soler, I. L. Garzon, and L. C. Balbas, Phys. Rev. B **70**, 165403 (2004).
[19] H. Hakkinen, M. Moseler, O. Kostko, N. Morgner, M. Hoffman, and B. Issendorff, Phys. Rev. Lett. **93**, 093401 (2004).
[20] H. Hakkinen, R. N. Barnett, and U. Landman, Phys. Rev. Lett. **82**, 3264 (1999).
[21] M. J. Frisch, G. W. Trucks, H. B. Schlegel, G. E. Scuseria, M. A. Robb, J. R. Cheeseman, J. A. Montgomery, Jr., T. Vreven, K. N. Kudin, J. C. Burant, J. M. Millam, S. S. Iyengar, J. Tomasi, V. Barone, B. Mennucci, M. Cossi, G. Scalmani, N. Rega, G. A. Petersson, H. Nakatsuji, M. Hada, M. Ehara, K. Toyota, R. Fukuda, J. Hasegawa, M. Ishida, T. Nakajima, Y. Honda, O. Kitao, H. Nakai, M. Klene, X. Li, J. E. Knox, H. P. Hratchian, J. B. Cross, V. Bakken, C. Adamo, J. Jaramillo, R. Gomperts, R. E. Stratmann, O. Yazyev, A. J. Austin, R. Cammi, C. Pomelli, J. W. Ochterski, P. Y. Ayala, K. Morokuma, G. A. Voth, P. Salvador, J. J. Dannenberg, V. G. Zakrzewski, S. Dapprich, A. D. Daniels, M. C. Strain, O. Farkas, D. K. Malick, A. D. Rabuck, K. Raghavachari, J. B. Foresman, J. V. Ortiz, Q. Cui, A. G. Baboul, S. Clifford, J. Cioslowski, B. B. Stefanov, G. Liu, A. Liashenko, P. Piskorz, I. Komaromi, R. L. Martin, D. J. Fox, T. Keith, M. A. Al-Laham, C. Y. Peng, A. Nanayakkara, M. Challacombe, P. M. W. Gill, B. Johnson, W. Chen, M. W. Wong, C. Gonzalez, and J. A. Pople, GAUSSIAN 03, Revision C.02, Gaussian, Inc., Wallingford, CT, 2004.
[22] F. Sue Legge, Graeme L. Nyberg, and J. Barrie Peel, J. Phys. Chem. A **105**, 7905–7916 (2001).
[23] D. Figgen, G. Rauhut, M. Dog, and H. Stoll, Chem. Phys. **311**, 227 (2005).
[24] K. A. Peterson and C. Puzzarini, Theor. Chem. Acc. **114**, 283 (2005).
[25] C. Gonzalez, Y. Simon-Manso, M. Marquez, and V. Mujica, J. Phys. Chem. B **110**, 687 (2006).
[26] J. P. Perdew, K. Burke, and M. Ernzerhof, Phys. Rev. Lett. **77**, 3865 (1996); **78**, 1396 (1997).
[27] A. D. Becke, J. Chem. Phys. **98**, 1372 (1993).
[28] D. Zanchet, H. Tolentino, M. C. Martins Alves, O. L. Alves, and D. Ugarte, Chem. Phys. Lett. **323**, 167 (2000).
[29] Certain commercial software is identified in this paper in order to specify the procedures adequately. Such identification is not intended to imply recommendation or endorsement by the National Institute of Standards and Technology, nor is it intended to imply that the materials or equipment identified are necessarily the best available for the purpose.
[30] P. Schwerdtfeger, J. R. Brown, J. K. Laerdahl, and H. Stoll, J. Chem. Phys. **113**, 7110 (2000).